

# Ionic Interactions at the Crude Oil–Brine–Rock Interfaces Using Different Surface Complexation Models and DLVO Theory: Application to Carbonate Wettability

Joel T. Tetteh,\* Richard Barimah, and Paa Kow Korsah



Cite This: *ACS Omega* 2022, 7, 7199–7212



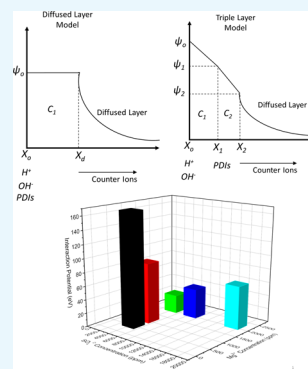
Read Online

ACCESS |

Metrics & More

Article Recommendations

**ABSTRACT:** The impact of ionic association with the carbonate surface and its influence toward carbonate wettability remains unclear and is an important topic of interest in the current literature. In this work, a triple layer model (TLM) approach was used to capture the electrokinetic interactions at both calcite–brine and oil–brine interfaces. The developed TLM was assembled against measured  $\zeta$ -potential values from the literature, successfully capturing the trends and closely matching the  $\zeta$ -potential magnitudes. The developed TLM was compared to a diffused layer model (DLM) presented in previous works, with the DLM showing a better match to the  $\zeta$ -potential values for seawater brine solutions. The  $\zeta$ -potential values predicted from both surface complexation models (SCMs) were used to calculate the total interaction energy (or potential) based on the Derjaguin, Landau, Verwey, and Overbeek (DLVO) theory. It was observed that low  $Mg^{2+}$  and high  $SO_4^{2-}$  concentrations in modified composition brine (MCB) made the calcite–brine interface more negative. However, at the oil–brine interface, low  $Mg^{2+}$  made the oil–brine interface more negative but high  $SO_4^{2-}$  concentrations slightly shifted the oil–brine  $\zeta$ -potential toward negative. At the crude oil–brine–rock (COBR) interfaces, low  $Mg^{2+}$  and high  $SO_4^{2-}$  concentrations in the MCB were observed to generate a greater repulsive interaction energy, which could trigger carbonate wettability alteration toward water wetness. The absolute sum of the  $\zeta$ -potential at both interfaces was observed to be correlated to the total interaction potential at a 0.25 nm separating distance. Thus, an increase in the absolute sum of the  $\zeta$ -potentials would generate a greater repulsive interaction potential and trigger wettability alteration. Therefore, these SCMs can be applied to design modified composition brine capable of triggering a repulsive interaction energy to alter carbonate wettability toward water wetness.



## 1. INTRODUCTION

The use of modified composition brine (MCB), also referred to as smart water, for waterflooding purposes has been explored for carbonate rocks in the recent literature.<sup>1–8</sup> However, the underlying mechanisms responsible for the observed improvement in oil production are still debatable. Mechanisms associated with rock wettability alteration from oil-wet to water-wet states have been proposed to cause improved oil recovery. Most carbonate rocks exhibit oil-wet nature mainly due to the positively charged calcite surface and the presence of negatively charged carboxylic materials in crude oil.<sup>9,10</sup> This hinders oil recovery from most carbonate rocks through usual waterflooding. The wettability alteration mechanisms associated with carbonate rocks are multivalent ionic exchange, expansion of the electrical double layer (EDL), electrostatic bond interactions, surface charge alteration, and calcite dissolution.<sup>11–15</sup> These mechanisms require the understanding of the electrostatic interaction at the rock surface caused by brine salinity and composition. The concept of potential determining ions (PDIs) influencing the wettability alteration process had been extensively investigated by Austad and co-workers in various publications for chalk formations.<sup>4,16,17</sup> They proposed

the multivalent ionic exchange process involving the PDIs (i.e.,  $Mg^{2+}$ ,  $Ca^{2+}$ , and  $SO_4^{2-}$ ) to be responsible for the wettability alteration leading to the improved oil recovery in chalk formations, stating that these ions need to be present in brine composition to observe improved oil recovery.<sup>16,18</sup> In various literature, reducing brine salinity and increasing  $SO_4^{2-}$  have been associated with shifting carbonate surface charge to negative, resulting in a repulsive disjoining pressure and altering the surface wettability toward a water-wet state.

Surface complexation models (SCMs) have taken a prominent stage in capturing the electrostatic effect of brine salinity and ionic adsorption on the calcite surface.<sup>11,14,19–27</sup> SCM provides molecular and thermodynamic descriptions of the electrostatic and geochemical interactions on a colloidal surface. Different types of SCM have been proposed in the

**Received:** December 8, 2021

**Accepted:** February 3, 2022

**Published:** February 15, 2022



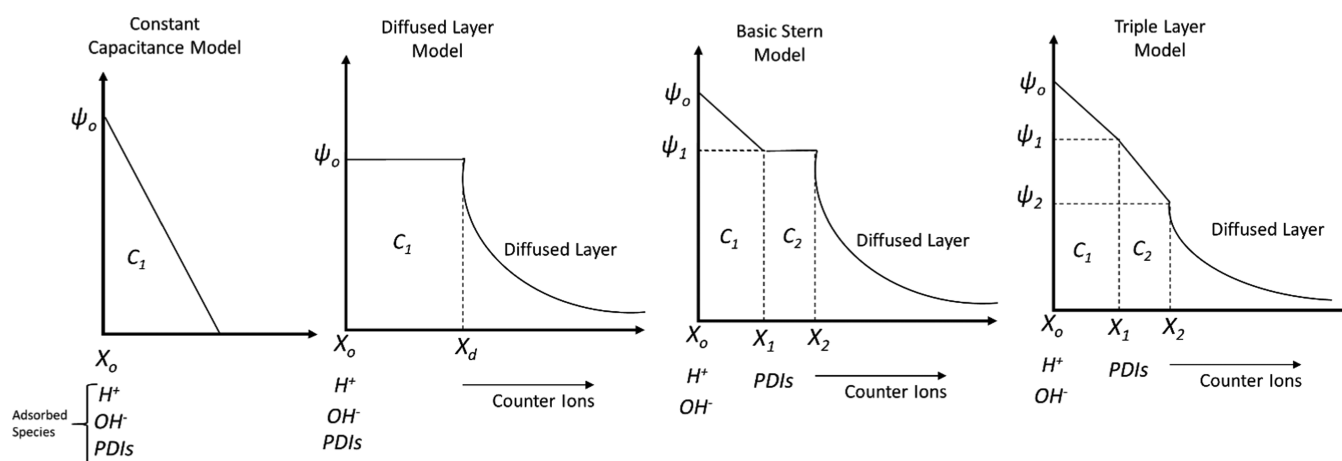


**Figure 1.** Schematic description of the solid–liquid interface for the different SCMs.

literature to describe the adsorption of ions on the colloidal surface.<sup>28,29</sup> Figure 1 shows the schematic describing the commonly used SCM for modeling the solid–liquid interface. The constant capacitance model (CCM) assumes ionic interaction at the inner Helmholtz plane of the solid–liquid interface, no background electrolytes at the diffused layer, and one plane with constant capacitance. The diffused layer model (DLM) behaves in a similar manner as the CCM. However, the DLM assumes background ions in the diffused layer to balance out the surface charge at the solid–liquid interface.<sup>28,29</sup>

The basic stern model (BSM) and the triple layer model (TLM) behave in a similar manner. Both models assume three parallel planes separated by defined capacitances at each plane. The capacitance is inversely related to the distance between the planes.<sup>30</sup> The calcite surface ( $X_0$ ) observes the chemisorption of the  $H^+$  and  $OH^-$  to the surface to form the hydration sites. The inner Helmholtz layer ( $X_1$ ) observes the adsorption of PDIs and the hydrated forms of the PDIs onto the outer Helmholtz layer ( $X_2$ ). The counter ions stay within the diffused layer to balance out the surface charge.<sup>31–34</sup> Assuming three planes for the calcite–brine interface seems to be an appropriate assumption for electrostatic interactions. Thus, the BSM- and the TLM-based SCMs should better represent the electrostatic ionic interactions at the calcite surface. However, the DLM-based SCM, which is simple to execute, does an adequate job to represent the calcite surface and match  $\zeta$ -potential measured.<sup>11,19,21,27,35</sup> Also, the location of the  $X_2$  plane can be altered and expanded to coincide with the slipping plane. In this case, the potential at the  $X_2$  plane could be assumed to be the same as the  $\zeta$ -potential.<sup>30</sup>

The SCM provides an insight into the role of electrostatic forces and interactions toward the total surface forces at the crude oil–brine–rock (COBR) interface. Brady et al.<sup>36</sup> combined both SCM and Derjaguin, Landau, Verwey, and Overbeek (DLVO) theory to indicate changes in sandstone rock wettability. Mahani et al.,<sup>2,12,37</sup> through a series of works, showed that SCM could be used to explain the role of electrostatic interactions toward the change in carbonate rock wettability when using MCB from the middle East. Sanaei et al.<sup>38</sup> and Bordeaux-Rego et al.<sup>39</sup> extended the application of SCM by combining their model with DLVO calculations of disjoining pressure to successfully predict the carbonate rock contact angle. It should also be noted that SCM has been combined with reactive flow models such as UTCHEM to predict oil recovery from formations.<sup>40–42</sup> These approaches

served to streamline both SCM and DLVO theory incorporated into reactive flow models to serve as a predictive tool for designing chemically tuned brine compositions.

It should be noted that the observation of improved oil recovery in rocks occurs over a series of length and time scales.<sup>5,43,44</sup> Across the length scale, SCM serves to provide an understanding of the rock–brine–oil interactions at the nanoscale, where the rock surface is considered as a smooth colloidal particle interacting with oil molecules. This technique neglects the role of surface roughness, which has been studied to influence carbonate rock.<sup>45,46</sup> In a work by Al Maskari et al.,<sup>45</sup> it was observed that surface roughness ( $\sim 17$  nm) caused by calcite dissolution did not greatly influence the wettability alteration trends caused by low salinity water on calcite substrates. Rather, Al Maskari et al.<sup>45</sup> proposed that the electrostatic interactions at the nanoscale were strong and served as the driver for the observed changes in calcite wettability. In further analysis aimed at increasing the surface roughness, Sari et al.<sup>46</sup> observed that at higher roughness ( $\sim 945$  nm), the wetting state of the calcite rock was affected. They observed that the changes in wettability due to surface roughness could not be predicted by the Wenzel contact angle model, indicating the importance of incorporating electrostatic interactions at different length scales for analysis. At the pore/microscale, microfluidic devices and micro-CT have been used to observe the mobilization of the oil molecules caused by wettability alteration and fluid–fluid interaction such as microdispersion formation and osmosis.<sup>47–52</sup> In a recent review by Liu et al.,<sup>53</sup> geochemistry was combined with a Lattice Boltzmann pore model to indicate how nanoscale observations from SCM could be translated to pore or microscale. The observations at the nano and microscales also translate to the observation of oil recovery at the macroscale through coreflooding experiments.<sup>5,54</sup> However, the time it takes for oil to be recovered during low salinity waterflooding has seldomly been treated in the literature. In a recent work by Pourakaberian et al.,<sup>55</sup> the wettability alteration process in porous media was observed to be slow due to the electrodiffusion of ions at the thin water film and its effect on the electrostatic forces. Similarly, by performing oil recovery experiment using a novel quasi-two-dimensional (2D) heterogeneous calcite micromodel, Mohammadi et al.<sup>49,51</sup> observed a slow wettability alteration process and a characteristic slow layer-by-layer oil peel-off from the pore walls, which impacted the oil recovery. Mohammadi et al.<sup>49,51</sup> suggested that a long shut period was required to generate significant wettability

**Table 1. Sorption Reactions and Constants (log *K*) Used in the DLM-Based SCM at 25 °C**

reaction		Brady et al. <sup>58</sup>	Tetteh et al. <sup>11</sup>	Ding and Rahman <sup>34</sup>	Sanaei et al. <sup>38</sup>	Bordeaux-Rego et al. <sup>39</sup>
>CaOH + H <sup>+</sup> ↔ >CaOH <sub>2</sub> <sup>+</sup>	1	11.85	11.85	11.8	11.6	11.3
>CaOH <sub>2</sub> <sup>+</sup> + SO <sub>4</sub> <sup>2-</sup> ↔ >CaSO <sub>4</sub> <sup>-</sup> + H <sub>2</sub> O	2	2.1	2.1	-2.1	2.1	1.1
>CaOH + HCO <sub>3</sub> <sup>-</sup> ↔ >CaCO <sub>3</sub> <sup>-</sup> + H <sub>2</sub> O	3	5.8	5.8		5.8	6.8
>CaOH <sub>2</sub> <sup>+</sup> + CO <sub>3</sub> <sup>2-</sup> ↔ >CaCO <sub>3</sub> <sup>-</sup> + H <sub>2</sub> O	4			6.0		
>CO <sub>3</sub> H ↔ >CO <sub>3</sub> <sup>-</sup> + H <sup>+</sup>	5	-5.1	-5.1	-5.1	-4.6	-4.36
>CO <sub>3</sub> H + Ca <sup>2+</sup> ↔ >CO <sub>3</sub> Ca <sup>+</sup> + H <sup>+</sup>	6	-2.6	-4.4		-2.6	-2.76
>CO <sub>3</sub> H + Mg <sup>2+</sup> ↔ >CO <sub>3</sub> Mg <sup>+</sup> + H <sup>+</sup>	7	-2.6	-4.4		-2.1	-1.6
>CO <sub>3</sub> H + Na <sup>+</sup> ↔ >CO <sub>3</sub> HNa <sup>+</sup>	8					3.7

alteration and layer-by-layer oil peel-off, which would result in oil bank build up for improved recovery. Similar works, both experimental and numerical, are required to advance the knowledge of the time dependence of the low salinity waterflooding effect in both sandstones and carbonates.

In this work, a review of the match fitting of the DLM-based SCM would be analyzed to establish the shortcoming of the model. This review would serve as a centralized location on the advancement of SCM for its application toward wettability alteration on carbonate rock using MCB. TLM was assembled against the experimental  $\zeta$ -potential for the calcite–brine and oil–brine interfaces and compared with the already developed DLM, which could be used as a first step in developing a more rigorous electrostatic model. This comparative analysis would show the advantages of the simpler DLM or the more rigorous TLM in predicting the electrostatic interactions at the carbonate surface. The assembled TLM was used to evaluate the impact of Mg<sup>2+</sup> and SO<sub>4</sub><sup>2-</sup> interacting at the crude oil–brine–rock (COBR) interface and its influence on carbonate wettability for the optimization of the brine chemistry. Total interaction energy (or potential) at the COBR interface was calculated based on the Derjaguin, Landau, Verwey, and Overbeek (DLVO) theory to assess the wettability alteration potential of MCB. It should be noted that this work neglects the effect of surface roughness and the time scale on the wettability alteration process. This work showed that MCB with low Mg<sup>2+</sup> and high SO<sub>4</sub><sup>2-</sup> could generate a slightly negative  $\zeta$ -potential at both oil–brine and calcite–brine interfaces, resulting in a greater repulsive interaction energy.

## 2. PREDICTING IONIC ADSORPTION ON CALCITE SURFACES USING DLM-BASED SCM

The geochemical, molecular, and thermodynamic interaction between aqueous species and colloidal surfaces can be described using SCM.<sup>5,14,56</sup> Rock surfaces can behave as colloidal surface dispersed in aqueous brine solutions.<sup>11</sup> The PHREEQC simulator developed by the USGS has been widely used to simulate surface complexations for rock minerals.<sup>56,57</sup> In recent years, SCM has been used to describe the electrostatic interaction between brine ions and the carbonate rock surface.<sup>11,12,14,15,21–23,26,38,39,58–64</sup> Brady et al.<sup>58</sup> developed an SCM to describe the calcite surface and investigate the potential changes in wettability caused by different brine compositions. They modeled the calcite surfaces as >CaOH and >CO<sub>3</sub>H hydration sites, which protonate or deprotonate to form positive and negative reactive species. This approach was universally adopted in the modeling of calcite surfaces in evaluating the electrokinetic properties.<sup>11,14,23,27</sup> Brady et al.<sup>58</sup> used reaction sorption constants analogous to the geochemical databases (Table 1) to predict the electrostatic interactions that influence the calcite–brine interface. However, Song et al.<sup>21</sup> developed a

DLM model using fractional charges for the hydrations sites. They argued that the entire surface of a calcite mineral was not exposed to electrostatic interaction with brine ions and hence represented the hydration sites as >CaOH<sup>-0.75</sup> and >CO<sub>3</sub>H<sup>+0.75</sup>. The SCM developed by Song et al. sufficiently predicted the  $\zeta$ -potential measured for the calcite–brine interface by adjusting the sorption constants. This different representation of the primary hydration sites could impact the electrokinetic surface properties predicted using the SCM and hence introduce more uncertainties in the modeling approach.

Another source of uncertainties in the SCM is the reaction sorption constants adopted for the modeling. Table 1 shows reactions typically used for DLM-based SCM in the literature and the adopted sorption constants. These sorption constants were either adopted from a geochemical database or after matching the  $\zeta$ -potential experiment data. Tetteh et al.,<sup>11</sup> Sanaei et al.,<sup>38</sup> and Bordeaux-Rego et al.<sup>39</sup> matched the measured  $\zeta$ -potential in the literature with the developed SCM by modifying the sorption constants. As indicated in Table 1, sorption constants used by different authors were different that could introduce uncertainty in model fitting. Eftekhari et al.<sup>65</sup> also observed in their thermodynamic analysis that the commonly used sorption constants in the literature were insufficient in predicting the measured  $\zeta$ -potential and hence new constants were adopted.

The site surface density of calcite surfaces has also been modified in the literature to match experimental data. Eftekhari et al.<sup>65</sup> varied the site density from 2 to 5 sites/nm<sup>2</sup> to match experimental data from Zhang et al.<sup>17</sup> Hiorth et al.<sup>15</sup> in matching their experimental data used a site density for calcite of 2 site/nm<sup>2</sup>. Mahani et al.<sup>12</sup> employed a calcite site density of 5 site/nm<sup>2</sup> in predicting the surface potential, which was used for wettability predictions. However, the calcite site density of 4.95 sites/nm<sup>2</sup> is most commonly used in predicting electrokinetic properties of calcite surfaces.<sup>11,21,26,27,31,34,63,66,67</sup> Thus, it would be appropriate to determine the active site density of calcite surfaces through experimental approaches to correctly match the model prediction.

Another aspect of consideration in modeling the ionic interactions at the COBR interface would be the effect of temperature. The low salinity effect on rock wettability improves at higher temperatures by triggering the increased activity of PDIs.<sup>16,19,23,68,69</sup> Thus, it would be very important to carefully consider the effect of temperature in SCM. Tetteh et al.<sup>19</sup> and Mansi et al.<sup>70</sup> modeled the effect of temperature on the electrostatic interactions at the sandstone and carbonate surfaces, respectively, using the van't Hoff equation and proposed reaction enthalpies. However, a limiting component of the van't Hoff equation is the unavailability of reliable data on the heat of reactions and enthalpies for the surface complexation reactions reported in the literature. Thus, in recent publications

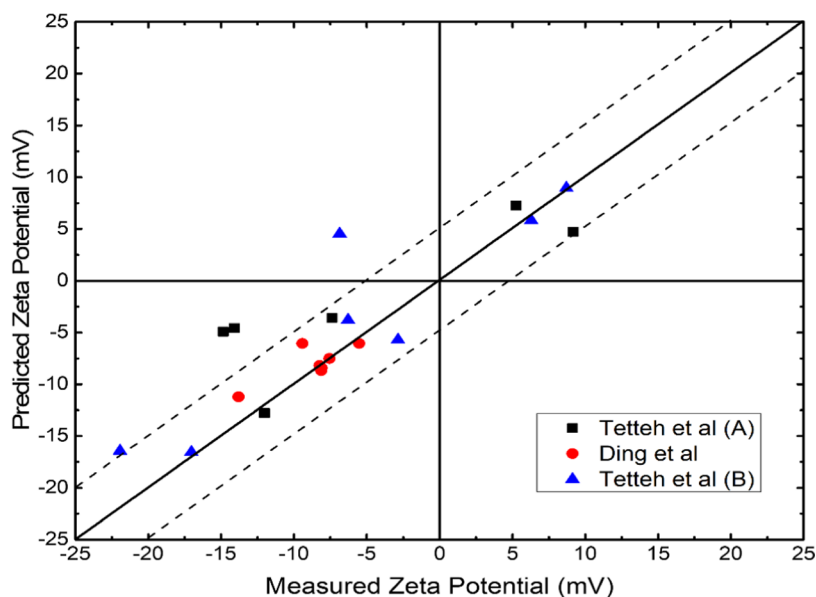


**Figure 2.**  $\zeta$ -Potential matching using DLM developed by Tetteh et al.<sup>11</sup> The model was used to predict  $\zeta$ -potential measured by Tetteh et al. (A),<sup>11</sup> Ding et al.,<sup>34</sup> and Tetteh et al. (B).<sup>27</sup> Data adapted with permission.

**Table 2.** Brine Composition Used for SCM and Disjoining Pressure Calculation<sup>a</sup>

ions, ppm	SW	SW2SO	SW4SO	SW0.2SMg	SW0.5Mg
Ca <sup>2+</sup>	650	650	650	650	650
Mg <sup>2+</sup>	2110	2110	2110	528	1055
Na <sup>+</sup>	18 300	20 356	24 467	18 300	18 300
Cl <sup>-</sup>	32 399	32 399	32 399	27 717	29 278
SO <sub>4</sub> <sup>2-</sup>	4290	8580	17160	4290	4290
IS, mol/L	1.118	1.194	1.358	0.933	0.993
total concentration of cations (mol/L)	1.0021	1.0915	1.2703	0.8719	0.9153
total concentration of anions (mol/L)	1.0032	1.0925	1.2711	0.8711	0.9151
charge balance (mol/L)	-0.0011	-0.0010	-0.0008	0.0008	0.0001

<sup>a</sup>Adapted with permission from Ding and Rahman, Energy and Fuel, 2018,<sup>34</sup> Copyright 2018, American Chemical Society.

by Khurshid and Alshalabi<sup>71</sup> and Korrani et al.,<sup>72</sup> a polynomial analytical solution was implemented to define the impact of temperature on the surface complexation reactions and their intrinsic reaction constants at higher temperatures, which was relevant to the reservoir system. This technique better represented the changes in temperature and the impact of electrostatic interactions at a higher temperature.

In previous works,<sup>11,27</sup> SCM was developed for predicting calcite–brine  $\zeta$ -potential measured. Reactions between calcite and brine ions used by Brady et al.<sup>14,58</sup> were adopted in DLM-based SCM predictions. The sorption constants used by Brady et al.<sup>14,58</sup> were modified to match the experimental data. The reactions describing the association of the divalent cations toward the calcite surface were modified to fit the experimentally measured  $\zeta$ -potential (Table 1). A calcite site density of 4.95 sites/nm<sup>2</sup> and a specific surface area of 1 m<sup>2</sup>/g were used in the model prediction.  $\zeta$ -Potential was predicted from the calculated surface potential by using the Debye Hückle approximation of the Poisson–Boltzmann equation.<sup>11,56,73</sup> Figure 2 shows the measured and predicted  $\zeta$ -potential of the calcite–brine interface using the DLM-based SCM. Root-mean-square error (RSME) for the model prediction was observed to be  $\pm 4.6$  mV. Thus, the DLM-based SCM provided a reasonable fit to the experimental data, considering the experimental uncertainties during measurement. In this work, the TLM-based SCM was

used to model the electrostatic interaction at the calcite–brine interface and compared with the already established DLM-based SCM. This approach would improve the understanding of the electrical double layer of the calcite lattice and the effect of ionic association on carbonate wettability. This approach would also enhance and elaborate the importance of ionic placement in the electrical double layer of both the oil–brine and calcite–brine interfaces, hence, appropriately indicating the species concentration on both interfaces.

### 3. MATERIALS AND METHOD

**3.1. Brine, Crude Oil, and Rock Material Used.** Brine composition from the literature was used for the model fitting and  $\zeta$ -potential prediction. In particular, brine composition from Ding and Rahman<sup>34</sup> was used for  $\zeta$ -potential matching and calculation of the interaction energy at the COBR interfaces and hence is shown in Table 2. In the brine composition listed in Table 2, SW represents seawater brine. The different SW brines with modified ionic composition were used to investigate the effect of Mg<sup>2+</sup> and SO<sub>4</sub><sup>2-</sup> ions on the electrostatic interactions. For example, SW0.5Mg and SW2SO represented seawater brine with half and twice the concentration of Mg<sup>2+</sup> and SO<sub>4</sub><sup>2-</sup> ions, respectively. In addition, brine compositions used by Magsoudian et al.<sup>74</sup> and Alshakhs and Kovscek<sup>75</sup> (Table A1) were used in the prediction of the calcite–brine and oil–brine

Table 3. Sorption Reaction, Constants (log *K*), and Charge Distribution Used for the TLM-Based SCM at 25 °C<sup>a</sup>

	reaction	$\Delta Z_0^*$	$\Delta Z_1^*$	$\Delta Z_2^*$	Log( <i>K</i> )
calcite–brine interface <sup>67,80,86,87</sup> site density = 4.95 sites/nm <sup>2</sup> , <sup>11,21,26,34</sup> specific surface area = 1 m <sup>2</sup> /g <sup>11,34</sup> )	$>\text{CaOH} + \text{H}^+ \leftrightarrow >\text{CaOH}_2^+$	1	0	0	11.85
	$>\text{CaOH}_2^+ + \text{SO}_4^{2-} \leftrightarrow >\text{CaSO}_4^- + \text{H}_2\text{O}$	0	-2	0	2.1
	$>\text{CaOH} + \text{HCO}_3^- \leftrightarrow >\text{CaCO}_3^- + \text{H}_2\text{O}$	0	-2	0	5.8
	$>\text{CO}_3\text{H} \leftrightarrow >\text{CO}_3^- + \text{H}^+$	-1	0	0	-5.1
	$>\text{CO}_3\text{H} + \text{Ca}^{2+} \leftrightarrow >\text{CO}_3\text{Ca}^+ + \text{H}^+$	-1	2	0	-4.4
	$>\text{CO}_3\text{H} + \text{Mg}^{2+} \leftrightarrow >\text{CO}_3\text{Mg}^+ + \text{H}^+$	-1	2	0	-4.4
oil–brine interface <sup>14,19,30,77</sup> (specific surface area = 1 m <sup>2</sup> /g, <sup>11,26</sup> refer to <sup>11,26,62</sup> for equation used for site density calculation)	$-\text{NH}^+ \leftrightarrow -\text{N} + \text{H}^+$	-1	0	0	-5.5
	$-\text{COOH} \leftrightarrow -\text{COO}^- + \text{H}^+$	-1	0	0	-4.6
	$-\text{COOH} + \text{Ca}^{2+} \leftrightarrow -\text{COOCa}^+ + \text{H}^+$	-1	2	0	-3.6
	$-\text{COOH} + \text{Mg}^{2+} \leftrightarrow -\text{COOMg}^+ + \text{H}^+$	-1	2	0	-3.4

<sup>a</sup>\*The  $\Delta Z_i$  values used in this work were based on the work by Hao et al.<sup>80</sup>

interfaces, respectively. Readers are referred to those manuscripts for brine composition. Crude oil compositions from Alshakhs and Kovscek<sup>75</sup> and Tetteh et al.<sup>11</sup> were used for the model predictions for the oil–brine interface. Rock composition with high calcite content was used for the modeling. Ding and Rahman measured  $\zeta$ -potential using Iceland spar with 98% calcite composition and was adopted in this paper. Due to the high calcite composition, the TLM-based SCM was considered a pure calcite surface.

**3.2. TLM-Based SCM Development.** Table 3 shows the detailed description of the TLM-based SCM. The TLM-based SCM was assembled using the charge distribution-multisite complexation model (CD-MUSIC), which is built into the PHREEQC software. In developing an SCM for a CORB interface, the rock surface was assumed to be interacting with aqueous solution, in this case, MCB to form a rock–brine interface. We assumed the oil molecule to interact with the aqueous phase whereby the oil molecules served as a smooth colloidal particle. This interaction also formed the oil–brine interface. The electrostatic interaction at the rock–brine interface was assembled using a pure and smooth calcite surface by assuming  $>\text{CaOH}$  and  $>\text{CO}_3\text{H}$  as the primary hydration sites.<sup>11,14,19,27,76</sup> For the oil–brine interface,  $-\text{COOH}$  and  $-\text{NH}$  were assumed as the hydration sites, representing the carboxylic and amine groups, respectively, of a crude oil molecule.<sup>11,27,30,58,77</sup> The charge distribution (Table 3), which indicated the placement of ions on different planes, was modeled similar to the approach by Ding and co-workers<sup>34,78</sup> and Heberling et al.,<sup>31,32</sup> for the calcite–brine interface, and Takeya et al.<sup>30</sup> for the oil–brine interface.  $\Delta Z_i$  value for each plane in the TLM was used to represent the transfer and sharing of net charge from one plane to the next based on the understanding of ionic placement in the calcite–brine and oil–brine planes. The protonation and deprotonation of the hydrations sites were assumed to occur at the hydrolysis layer,<sup>79</sup> which corresponded to the 0-plane or the inner plane, hence the net charge values assigned to  $\Delta Z_0$ ,  $\text{Ca}^{2+}$  and  $\text{Mg}^{2+}$  ions, which are known to strongly interact at the COBR interface, were assumed at the inner layer, with a net charge transfer to the outer layer (1-plane or  $\Delta Z_1$ ). The values used for the  $\Delta Z_i$  in Table 3 were sourced from the work by Hao et al.,<sup>80</sup> which were based on the understanding of the calcite–brine lattice.<sup>30,67,79–82</sup> The calcite–brine interface was equilibrated with calcite mineral and atmospheric  $\text{CO}_2$ , i.e., partial pressure of  $10^{-3.4}$  atm. However, the oil–brine interface was only equilibrated with atmospheric  $\text{CO}_2$ . The final pH value of the dispersion solution

was adjusted by adding different moles of HCl/NaOH, similar to the approach used in the literature.<sup>11,12,27</sup>

In the TLM-based SCM, the surface charge density in the diffused layer ( $\sigma_{\text{DL}}$ ) is computed from the Guoy–Chapman equation as<sup>56</sup>

$$\sigma_{\text{DL}} = -0.1174I^{0.5} \sinh\left(\frac{F\psi_2}{2RT}\right) \quad (1)$$

where  $F$  is Faraday's constant,  $R$  is the universal gas constant, and  $T$  is the absolute temperature.

The sum product of the species concentration ( $m_s$ ) and charge of the surface complexes ( $v_{\text{si}}$ ) based on protonation and deprotonation reactions between the colloidal surfaces (rock or oil molecule) and the aqueous species would result in the charge density at the diffused layer<sup>12</sup> (eq 2).

$$\sigma_{\text{DL}} = \frac{F}{AS} \sum m_s v_{\text{si}} \quad (2)$$

where  $A$  is the specific surface area (m<sup>2</sup>/g) of the particle;  $S$  is the solid concentration (g/L); and  $m_s$  is the concentration of surface species (mol/m<sup>2</sup>).<sup>12</sup> Surface species concentrations were calculated from mass action equations based on a series of presumed surface reactions and their equilibrium constants, as presented in Table 3.

The capacitance values were used to determine the potential at each plane based on a linear relationship with charge density, as indicated below.<sup>34</sup>

$$\sigma_0 = C_1(\psi_0 - \psi_1) \quad (3)$$

$$\sigma_0 + \sigma_1 = C_2(\psi_1 - \psi_2) \quad (4)$$

where  $\sigma_i$  and  $\psi_i$  represent the charge density (C/m<sup>2</sup>) and the potential (mV), respectively, at plane  $i$ . The potential at the 0-plane ( $\psi_0$ ) and 2-plane ( $\psi_2$ ) corresponds to the surface potential and the  $\zeta$ -potential based on the similar assumption by Takeya et al.<sup>30,67,77</sup> For the calcite–brine interface,  $C_1$  and  $C_2$  were assumed to be 1.3 and 4.5 F/m<sup>2</sup>, respectively.<sup>63,83</sup>  $C_1$  and  $C_2$  of 3.1 and 2.25 F/m<sup>2</sup>, respectively, were assumed for the oil–brine interface similar to the approach adopted by Takeya et al.<sup>30</sup> Vinogradov et al.<sup>84</sup> developed a relationship that showed the dependence of the capacitance value to the ionic strength of the brine used. In this work, since the ionic strengths of the brines used were in the range of seawater ( $\sim 1.1$  M), it was justifiable to use a constant capacitance for the calculations. More details on the relevant equations in the TLM model can be found in the literature.<sup>34,78,85</sup> The DLM presented in this work had been

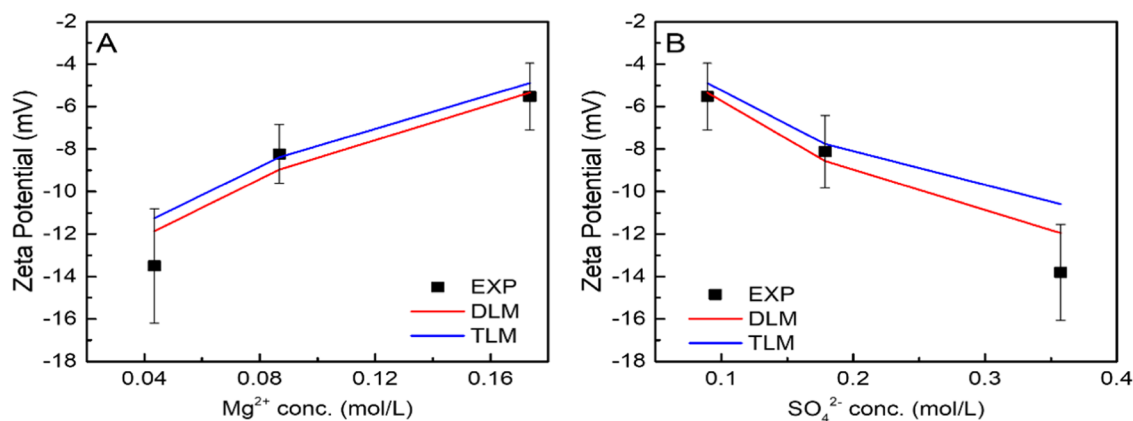


**Figure 3.** Prediction of calcite–brine  $\zeta$ -potential using both SCMs. (A) SW, SW0.5Mg, and SW0.25Mg brines were used for the species calculations to represent the variations in  $\text{Mg}^{2+}$  ion concentrations. (B) SW, SW2SO, and SW4SO brines were used for the species calculations to represent the variations in  $\text{SO}_4^{2-}$  ion concentrations. Solution pH was fixed at 8 for all calculations. Data adapted with permission from Ding and Rahman.<sup>34</sup>

shown in our previous publications with all of the relevant reactions and equations.<sup>11,19,27</sup>

**3.3. Interaction Energy at the COBR Interface: DLVO Theory.** The thermodynamic stability of the water film separating the crude oil molecules from the rock surface can be described by using the Derjaguin, Landau, Verwey, and Overbeek (DLVO) theory and hence was used in this work.<sup>5,88–91</sup> To determine the wetting state of a rock surface in the presence of water, the oil–brine interface was assumed to interact with the rock–brine interface resulting in an interaction energy at the COBR interface. Thus, to wet the rock surface with oil in the presence of a thin water film, the interaction energy must be overcome, causing the oil molecule to interact with the rock surface, resulting in oil wetness. As described in the literature,<sup>73,88,92</sup> the interaction force between two colloidal surfaces (assuming rock and oil colloidal surfaces) and separated by a wetting film (assuming brine) at a distance “ $h$ ” is related to the free energy ( $W$ ) per unit area. The summation of the van der Waals (vdW), electrical double layer (EDL), and the structural ( $S$ ) free energies made up the total interaction energy, as shown below<sup>73,88,92</sup>

$$W(h) = W_{\text{vdW}}(h) + W_{\text{EDL}}(h) + W_s(h) \quad (5)$$

Disjoining pressure at the COBR interface could be derived from the derivative of the total interaction energy per unit area with respect to the water film thickness ( $h$ ) in a direction normal to both interacting colloidal bodies.<sup>88</sup>

The vdW force, which is attractive and dominates the interaction forces closer to the surface, was calculated for a plate–plate geometry using the Lifshitz theory, as shown below<sup>88,93</sup>

$$W_{\text{vdW}}(h) = \frac{A}{12\pi h^2} \quad (6)$$

where “ $A$ ” is the Hamaker constant.<sup>93</sup> The EDL interaction free energy was calculated by assuming a constant potential–constant potential (CP–CP) boundary condition for solving the Poisson–Boltzmann equation.<sup>88</sup> This boundary condition provided an appropriate approximation of the analytical solution for the COBR interface.<sup>88,89</sup> Thus, the EDL interaction energy was calculated using eq 7 below<sup>88,92</sup>

$$W_{\text{EDL}}(h) = \frac{\epsilon \epsilon_w k [2\zeta_1 \zeta_2 - (\zeta_1^2 + \zeta_2^2) e^{(-kh)}]}{2 \sinh(kh)} \quad (7)$$

where  $\zeta_1$  and  $\zeta_2$  are the  $\zeta$ -potential of the calcite–brine and crude oil–brine interfaces, respectively,  $\epsilon_w$  is the relative permittivity of water,  $\epsilon$  is the absolute permittivity of the vacuum,  $8.854 \times 10^{-12}$  F/m,<sup>94,94</sup> and  $k$  is the inverse of Debye length at the calcite/oil–brine interfaces. The Hamaker constant of  $2.45 \times 10^{-21}$  J was used for calculating the vdW forces based on relative permittivity values and Lifshitz theory.<sup>89,94</sup> The structural interaction energy was ignored in the calculation similar to the approach by Mahani et al.<sup>88</sup> The structural forces were neglected because they were assumed to be sensitive at a very small separating distance from the colloidal surface.<sup>59,75</sup> A negative total interaction energy indicated a negative total disjoining pressure and hence corresponded to an attraction between the oil–brine and rock–brine interfaces. This would result in an oil-wet state on the calcite surface. However, a positive total interaction energy indicated a repulsive disjoining force between the oil–brine and rock–brine interfaces, corresponding to water wetness at the calcite surface.

## 4. RESULTS AND DISCUSSION

**4.1. Effect of  $\text{Mg}^{2+}$  and  $\text{SO}_4^{2-}$  on the Calcite–Brine Interface Using SCM.** Figure 3 shows the  $\zeta$ -potential prediction of the experimental data by Ding and Rahman.<sup>34</sup> The TLM in this work was compared to DLM previously developed in other publications<sup>11,19,27</sup> to show the fit to the experimental calcite–brine  $\zeta$ -potential. Both TLM and DLM closely predicted the trends and magnitude of measured calcite–brine  $\zeta$ -potential with respect to increasing  $\text{Mg}^{2+}$  and  $\text{SO}_4^{2-}$  concentrations in seawater-like brines. It could be observed that the increasing  $\text{Mg}^{2+}$  and  $\text{SO}_4^{2-}$  concentrations increased and decreased the predicted calcite–brine  $\zeta$ -potential, respectively. Similar observations were shown in the calcite–brine  $\zeta$ -potential predictions for Maghsoudian et al.,<sup>74</sup> as shown in Figure 4. Both TLM- and DLM-based SCMs predicted  $\zeta$ -potential trends for Maghsoudian et al.<sup>74</sup> but could not capture the magnitude of the  $\text{Mg}^{2+}$  adsorption on the calcite–brine interface. Nevertheless, the  $\text{Mg}^{2+}$  ion was observed to make the calcite–brine interface more positive, while the  $\text{SO}_4^{2-}$  ion made the calcite–brine interface more negative.

The speciation concentrations at the calcite–brine interface were investigated using the TLM-based SCM to shed more light on the ionic adsorption at the calcite surface (Figure 5). The increased adsorption of both  $\text{Mg}^{2+}$  and  $\text{SO}_4^{2-}$  ions ( $>\text{CO}_3$   $\text{Mg}^+$  and  $>\text{CaSO}_4^-$  species, respectively) at the calcite surface

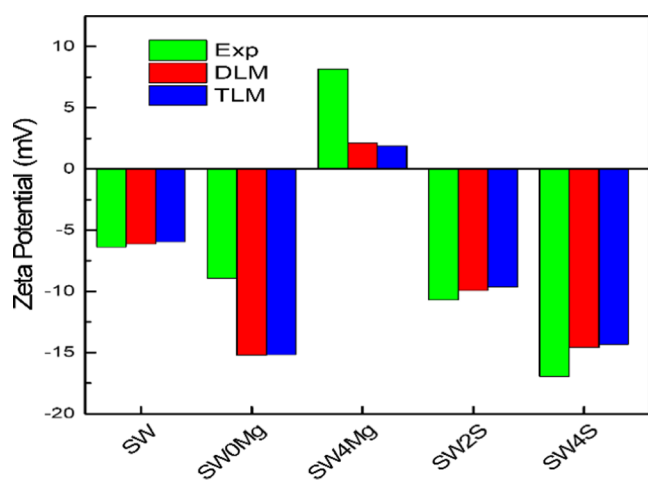


**Figure 4.** Prediction of calcite–brine  $\zeta$ -potential measured by Maghsoudian et al.<sup>74</sup> using both SCMs. Data adapted with permission from Maghsoudian et al.<sup>74</sup>

resulted in the reduction of the concentration of the dominant species ( $>\text{CaOH}_2^+$  and  $\text{CO}_3^-$  species). These observations in this work were similar to the work by Brady et al.<sup>14</sup> and Mahani et al.,<sup>12</sup> whereby  $\text{SO}_4^{2-}$  ion adsorption was observed to reduce the concentration of the  $>\text{CaOH}_2^+$  and hence making the calcite surface less oil-wet. As the concentration of  $\text{Mg}^{2+}$  and  $\text{SO}_4^{2-}$  ions increased in the aqueous phase, their interaction with the calcite surface resulted in consumption of the primary hydration sites ( $>\text{CaOH}$  and  $>\text{CO}_3\text{H}$ ) through their adsorption reactions. This caused a decrease in the concentration of the primary hydration sites and hence drove down the concentration of  $>\text{CaOH}_2^+$  and  $>\text{CO}_3^-$  species. The adsorption of  $\text{Mg}^{2+}$  on the calcite surface would promote the reactivity of  $\text{SO}_4^{2-}$  with the calcite surface (and vice-versa) to maintain the thermodynamic stability of the double layer, hence  $>\text{CO}_3\text{Mg}^+$  and  $>\text{CaSO}_4^-$  species increased in Figure 5.

At higher concentrations of  $\text{SO}_4^{2-}$  ions, the concentration of  $>\text{CO}_3^-$  was observed to be higher than that of  $\text{CaOH}_2^+$  (Figure 5B). Also, the concentration of  $>\text{CaSO}_4^-$  was observed to be higher than that of  $\text{CO}_3\text{Mg}^+$  with increasing  $\text{SO}_4^{2-}$

concentration. Both these observations would increase the difference between negative and positive species concentrations, shifting the total surface concentration toward negative and hence explained the observation of a decrease in  $\zeta$ -potential with the increasing  $\text{SO}_4^{2-}$  ion concentration (Figure 3B). On the other hand, the increasing  $\text{Mg}^{2+}$  concentration decreased the difference between the negative and positive species concentrations, hence making the calcite surface more positive, as indicated in (Figure 3A)

#### 4.2. Predicting $\zeta$ -Potential at the Oil–Brine Interface Using TLM-Based SCM.

$\zeta$ -Potential for the oil–brine interface measured by Alshakhs and Kavscek<sup>75</sup> was predicted using the reactions and equilibrium sorption constants in Table 3. The crude oil had a total acid number (TAN) and total base number (TBN) of 1.15 and 1.25 mg KOH/g, respectively. The site densities for the amine ( $-\text{N}$ ) and the carboxylic ( $-\text{COOH}$ ) groups were calculated to be 12.34 and 13.41 site/nm<sup>2</sup> based on calculations using the TAN and the TBN, respectively.<sup>11,26,62</sup>

The brine compositions used for the calculations could be found in Alshakhs and Kavscek.<sup>75</sup> Figure 6 shows that the TLM-based SCM captured the  $\zeta$ -potential trends and closely matched the magnitude of the measured  $\zeta$ -potential. Takeya et al.<sup>30,77</sup> assembled a TLM-based SCM to match the measured  $\zeta$ -potential of the oil–brine interface. They considered the carboxylic acid as the dominant and only primary hydration site at the oil–brine interface since the carboxylic acid strongly correlated to the electrokinetic at the oil–brine interface. However, in this work, the amine and carboxylic groups were modeled as a hydration site and hence resulted in a good match to the experimentally measured oil–brine  $\zeta$ -potential. Other works have incorporated the amine groups in modeling the electrokinetics at the oil–brine interface; however, the DLM-based SCM approach was employed.<sup>11,19,23,26,35,39,58,62,83,95</sup>

Oil–brine  $\zeta$ -potential was predicted using the brine composition from Ding and Rahman.<sup>34</sup> The brine composition used herein was the same as that used in Figure 3 to analyze the effect of  $\text{Mg}^{2+}$  and  $\text{SO}_4^{2-}$  at the calcite–brine interface. The crude oil composition used was similar to that used by Tetteh et al.<sup>11</sup> with TAN and TBN of 0.17 and 0.11 mg KOH/g. Thus, the oil–brine site densities were calculated to be 1.82 and 1.18 sites/nm<sup>2</sup>. It was observed from the oil–brine  $\zeta$ -potential predictions

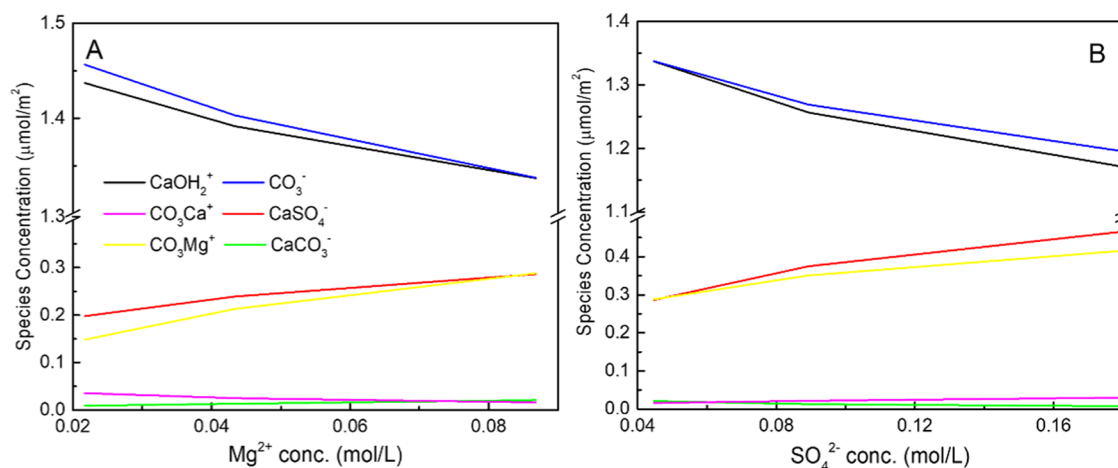


**Figure 5.** Predicting species concentration at the calcite–brine interface with respect to  $\text{Mg}^{2+}$  and  $\text{SO}_4^{2-}$  concentrations using the TLM-based SCM. (A) SW, SW0.5Mg, and SW0.25Mg brines were used for the species calculations to represent the variations in  $\text{Mg}^{2+}$  ion concentrations. (B) SW, SW2SO, and SW4SO brines were used for the species calculations to represent the variations in  $\text{SO}_4^{2-}$  ion concentrations. Brine composition from Ding and Rahman.<sup>34</sup>

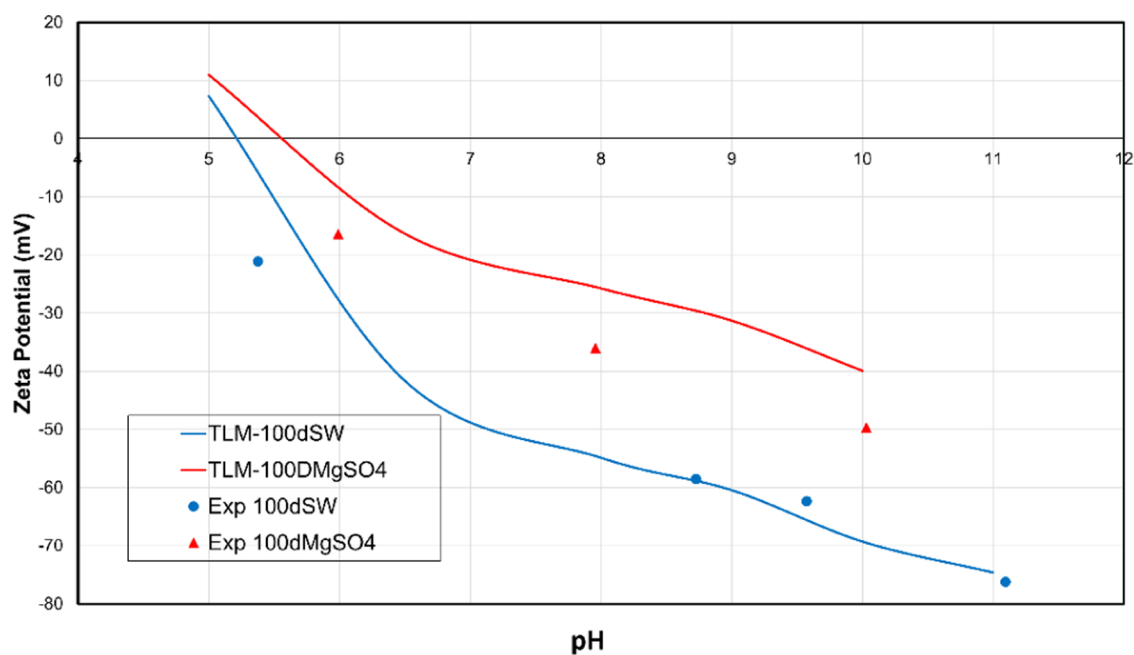


Figure 6. TLM prediction of oil–brine  $\zeta$ -potential. Data adapted with permission from Alshakhs and Kavscek.<sup>75</sup>

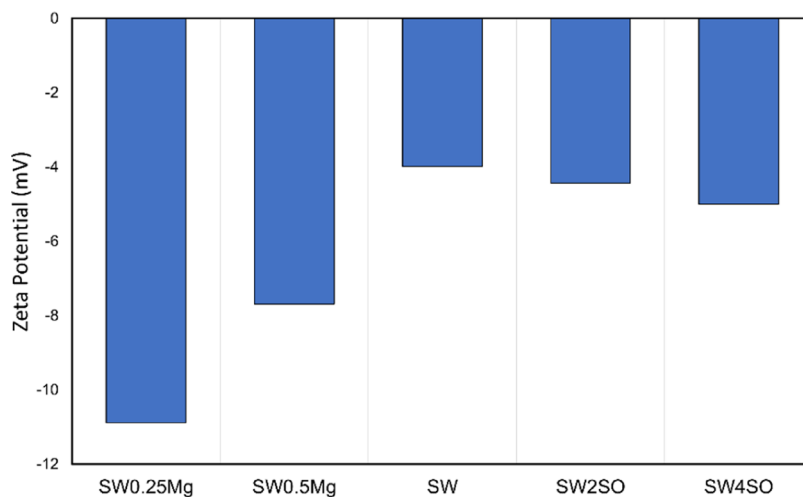


Figure 7. TLM prediction of oil–brine  $\zeta$ -potential using brine composition by Ding and Rahman.<sup>34</sup> Crude oil used had a TAN and TBN of 0.17 and 0.11 mg KOH/g taken from Tetteh et al.<sup>11</sup>

that increasing  $\text{Mg}^{2+}$  concentration increased the  $\zeta$ -potential, shifting the polarity toward positive (Figure 7). This could be attributed to the increased  $-\text{COOMg}^+$  species at the oil–brine interface due to the increased  $\text{Mg}^{2+}$  concentration in the brine. However, the increasing  $\text{SO}_4^{2-}$  concentration slightly decreased the  $\zeta$ -potential of the oil–brine interface, making the interface more negative.  $\text{SO}_4^{2-}$  was assumed to be nonreactive at the oil–brine interface and hence was not included in the sorption reaction. Thus, the formation of aqueous species associated with the  $\text{SO}_4^{2-}$  ions would reduce the positive ionic association at the oil–brine interface, making the oil–brine interface slightly more negative. This effect would impact the  $\zeta$ -potential at the oil–brine interface only slightly (Table A1).

#### 4.3. Thermodynamic Stability of the COBR Interface.

The wettability state in a rock porous media is known to be influenced by the thermodynamic stability of the COBR interface.<sup>5,43,75,96</sup> Carbonate rock wettability is a factor of the direct and indirect adsorption of crude oil molecules onto the

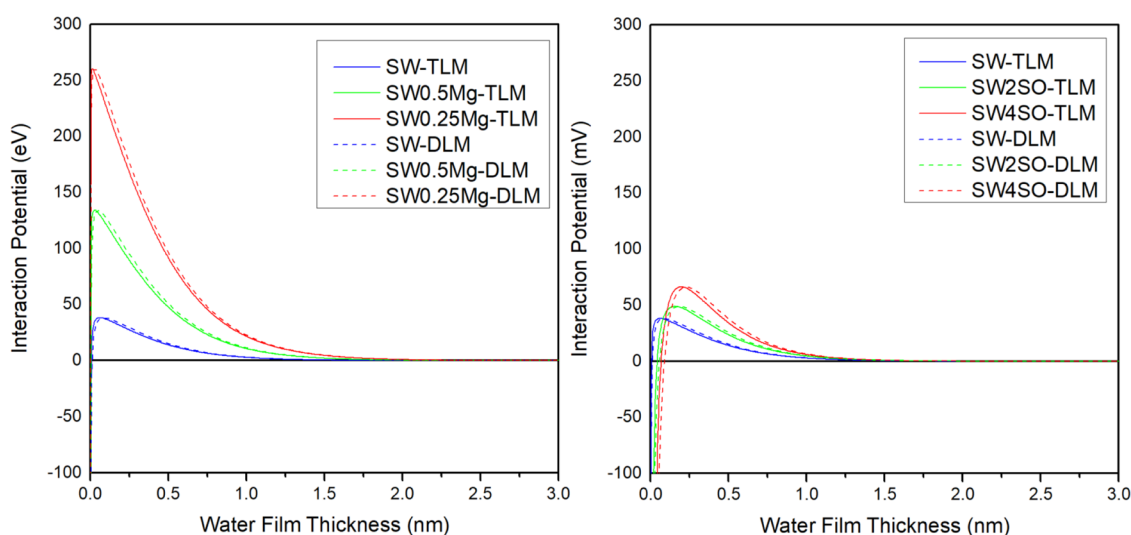
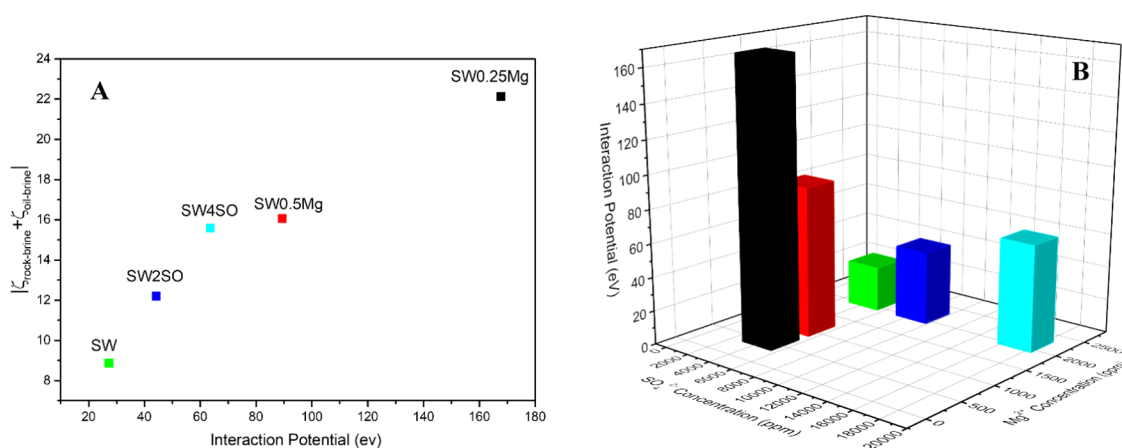
carbonate surface.<sup>14</sup> Direct crude oil adsorption on the carbonate surface could be attributed to the collapse of the water film known to be formed on the rock surface before oil migration. Thus, the crude oil molecules would have direct electrostatic interaction with the rock surface, which would result in a strongly oil-wet surface. On the other hand, the thermodynamic stability of the water film between the crude oil and rock surface would influence the indirect adsorption of the crude oil molecules toward the rock surface and hence impact carbonate rock wettability. The stability of the water film and the prediction of the wettability state on a rock surface have been previously evaluated in the literature using the bond product sum,<sup>11,14,19,23,27</sup> wetting film stability number,<sup>72</sup> the available adsorption sites,<sup>63</sup> and total disjoining pressure calculations.<sup>35,67</sup> In this section, the total interaction energy (or potential), which is directly related to the total disjoining pressure, was used to evaluate the impact of  $\text{Mg}^{2+}$  and  $\text{SO}_4^{2-}$  ions on the stability of the water film, impacting carbonate wettability. Calcite–brine  $\zeta$ -



**Table A1.** Brine Composition from Maghsoudian et al.<sup>74</sup> and Alshakhs and Kovscek<sup>75</sup> Used for the SCM and Interaction Energy Calculation<sup>a</sup>

ions, ppm	SW	SW2S	SW4S	SW0Mg	SW4Mg	100dSW	100dMgSO <sub>4</sub>
Ca <sup>2+</sup>	460	460	460	460	460	0	0
Mg <sup>2+</sup>	1530	1530	1530	0	6120	21	35
Na <sup>+</sup>	12 290	12 205	11 544	14 893	5464	172	102
Cl <sup>-</sup>	22 652	19 527	13 768	21 579	24 888	310	225
SO <sub>4</sub> <sup>2-</sup>	3210	6420	12840	3210	3210	43	89
K <sup>+</sup>	280	280	280	280	280	0	0
HCO <sup>-</sup>	122	150	150	150	150	0	0
TDS, ppm	40 572	40 572	40 572	40 572	40 572	546	451
IS, mol/L	1.291	1.233	1.108	1.311	1.246	0.0107	0.01008
total concentration of cations (mol/L)	0.6906	0.6869	0.6582	0.6779	0.7714	0.0092	0.0073
total concentration of anions (mol/L)	0.7058	0.6845	0.6557	0.6755	0.7689	0.0096	0.0082
charge balance (mol/L)	-0.0152	0.0024	0.0025	0.0024	0.0025	-0.0004	-0.0009

<sup>a</sup>IS and TDS represent the brine ionic strength and total dissolved solids, respectively. Data was adopted with permission from Maghsoudian et al. Journal of Molecular Liquid 2020,<sup>74</sup> Copyright 2020, Elsevier and Alshakhs and Kovscek,<sup>75</sup> Advances in Colloid and Interface Science, 2016, Copyright 2016, Elsevier.

**Figure 8.** Effect of Mg<sup>2+</sup> and SO<sub>4</sub><sup>2-</sup> ions on the interaction potential (energy) at the crude oil–brine interface, impacting carbonate wettability.**Figure 9.** (A) Relationship between total interaction potential (energy) and absolute  $\zeta$ -potential sum (with the same polarity) at oil–brine and rock–brine interfaces. (B) Relationship between total interaction potential (energy), Mg<sup>2+</sup> and SO<sub>4</sub><sup>2-</sup> concentrations in the seawater brine. Total interaction potential (energy) values at 0.25 nm water film thickness as used.

potential in Figure 3 and oil–brine  $\zeta$ -potential in Figure 7 were used for calculating the total interaction energy. The brine composition from Ding and Rahman<sup>34</sup> displayed in Table 2 was

used. In general, the DLM-based SCM predicted a higher interaction potential when compared with TLM-based SCM. This could be attributed to the difference in the prediction of the

rock–brine  $\zeta$ -potential when using different models (Figure 3). However, the differences in the calculated interaction potential using both models were negligible, and the observed trends were the same. Nevertheless, it is important to choose the appropriate SCM in predicting the electrostatic interactions at the COBR interface. By observing the trends in the interaction potential calculations, increasing the  $\text{SO}_4^{2-}$  concentration and decreasing the  $\text{Mg}^{2+}$  concentration increased the repulsive interaction energy at the COBR interface (Figure 8). However, the  $\text{Mg}^{2+}$  ion had a greater impact on influencing the interaction energy at the COBR interface. Low  $\text{Mg}^{2+}$  concentration (SW0.25Mg, 528 ppm) resulted in the greatest repulsive interaction potential ( $\sim 260$  eV) at the COBR interface. This could be attributed to the reactivity of the oil–brine and calcite–brine interfaces to the  $\text{Mg}^{2+}$  ion. Reducing  $\text{Mg}^{2+}$  ion concentration shifted the  $\zeta$ -potential toward more negative at both interfaces, hence resulting in the expansion of the double layers at both oil–brine and calcite–brine interfaces, which would alter rock wettability toward water wetness. However, increasing  $\text{SO}_4^{2-}$  concentration had a greater impact on the calcite–brine interface than the oil–brine interface, affecting the changes in the interaction energy.

To further validate the impact of the predicted  $\zeta$ -potential on the total interaction potential calculations, the absolute sum of the  $\zeta$ -potential at both interfaces was determined (Figure 9). Interaction potential at 0.25 nm was used because water film thickness between oil molecules and rock surface had been calculated using molecular dynamic simulation and measured to be between 0.15 and 0.25 nm.<sup>97,98</sup> It should be noted that water film thickness is a function of brine ionic strength, brine composition, and rock type used.<sup>90</sup> However, in this work, brines with very similar ionic strength (seawater ionic strength  $\sim 1$  M) were used, the rock type was purely calcite, and the oil composition was the same. Hence, the use of 0.25 water film thickness to assess the trends of wettability alteration may be an adequate assumption. Figure 9 shows that the absolute sum of predicted  $\zeta$ -potential at both interfaces trended well with the magnitude of the interaction energy required to collapse the water film at the COBR interface. The greater the absolute sum, the higher the interaction energy at the COBR interface. Similar observations were made by Sari et al.,<sup>99</sup> whereby the greater the absolute sum of  $\zeta$ -potential at both interfaces, the lower the measured contact angle and hence a more water-wet calcite surface. This supported the reliability of the analysis with respect to the absolute sum of  $\zeta$ -potential at both interfaces. Thus, increasing the magnitude of the  $\zeta$ -potential at both interfaces had the potential of generating a higher repulsive force and hence altered the carbonate surface wettability toward water-wet. SW0.25Mg triggered a greater magnitude of  $\zeta$ -potential at both interfaces and hence generated the greatest repulsive interaction energy at the COBR interface. However, even though the SW4SO triggered a higher magnitude of calcite–brine  $\zeta$ -potential but slightly impacted the oil–brine  $\zeta$ -potential, the total interaction energy was lower than that of SW0.25Mg. Based on this analysis, the order of increasing repulsive interaction potential was SW < SW2SO < SW4SO < SW0.5Mg < SW0.25Mg. Therefore, seawater brine with low  $\text{Mg}^{2+}$  and high  $\text{SO}_4^{2-}$  concentration would trigger high repulsive interaction energy and hence alter carbonate rock wettability toward water wetness. The observation herein was consistent to contact angle measurements performed by Ding et al.<sup>100</sup> using the same brine composition. Ding et al.<sup>100</sup> observed that a decrease in  $\text{Mg}^{2+}$  concentration impacted the wettability

alteration process that an increase in  $\text{SO}_4^{2-}$  concentration. SW0.25Mg resulted in the contact angle of  $85.3^\circ$  as compared to the SW4S measuring contact angle of  $98.6^\circ$ . However, both modified composition brines measured a low contact angle as compared to SW brine ( $118^\circ$ ). It should however be noted that mineral oil instead of crude oil was used for the contact angle measurement.<sup>100</sup> The adsorption of ions toward the oil–brine interface when using mineral oil remains unknown and hence was not modeled using the TLM-based SCM. Nevertheless, the trends of the effect of  $\text{Mg}^{2+}$  and  $\text{SO}_4^{2-}$  ions on carbonate wettability in the work by Ding et al.<sup>100</sup> were consistent with the total interaction potential calculated herein. It should be noted that both  $\text{Mg}^{2+}$  and  $\text{SO}_4^{2-}$  ions have the potential to form scales and damage the reservoir formation.<sup>5,101–103</sup> However, Figure 9 indicates that the MCB with the lowest  $\text{Mg}^{2+}$  and  $\text{SO}_4^{2-}$  ions (SW0.25Mg brine) has the potential to result in the greatest wettability alteration and hence the improved oil recovery. It is thus important that scaling potential geochemical analysis be performed for all MCB, together with SCM and DLVO theory calculations to fully assess the potential of MCB for field applications.

It is noteworthy to state that the TLM assembled against experimental data in this work had some limitations. The simplified DLM provided a slightly better match to the experimental data at the ionic strength used for this work. This indicated that further experimental research is required to identify the locations of the brine ions in the planes and the experimentally determined capacitance between planes. Furthermore, the reaction sorption constants may be different in the TLM based on the proximity of the ionic association with the colloidal surface, hence there is a need for further electrokinetic measurements. Thus, it should be noted that for simple low salinity brines (below  $\sim 1$  M) the use of the much simpler DLM could provide a quicker and more accurate approximation of the electrostatic interactions at the COBR interface. This work did not investigate the effect of increasing  $\text{Ca}^{2+}$  on carbonate wettability. However,  $\text{Ca}^{2+}$  has been investigated over the years as a very active PDI on the carbonate surface, greatly impacting surface wettability.<sup>5,13,104</sup> The modeling of the effect of  $\text{Ca}^{2+}$  on carbonate wettability should be coupled with the effect of calcite dissolution, rendering the process complicated. In most experimentally measured  $\zeta$ -potential, the procedure used could result in different measures of calcite dissolution, which would greatly impact the magnitude of the  $\zeta$ -potential. Thus, the most suitable way of modeling the effect of  $\text{Ca}^{2+}$  would be by comparing the measured dissolved  $\text{Ca}^{2+}$  after dispersion with that predicted by the geochemical model and also matched with the  $\zeta$ -potential. This research effort is currently being undertaken for future publications. The effect of higher ionic strength (above 2 M) on the assembled TLM also needs further investigation. Initial modeling efforts by Vinogradov et al.<sup>84</sup> have all shown the added advantage of using the TLM for modeling the electrokinetic interactions of a high ionic strength brine solution. It should be noted that this TLM assembled herein against experimental data in the literature serves as a first step in the development of a more rigorous electrostatic model. Therefore, more experimental results are required to adequately model the effect of high ionic strength and PDIs on both the oil–brine and calcite–brine interfaces.

## 5. CONCLUSIONS

In this work, the electrokinetic properties of the calcite–brine and the oil–brine interface were predicted using the TLM. At

the calcite–brine interface, the TLM was assembled against experimentally measured  $\zeta$ -potential in the literature and compared to previously developed DLM. A summary of predicted  $\zeta$ -potential from the DLM-based SCM model was also provided. For the oil–brine interface, the TLM was assembled against measured  $\zeta$ -potential from Alshakhs and Kovscek.<sup>75</sup> The impact of  $\text{Mg}^{2+}$  and  $\text{SO}_4^{2-}$  ions toward the electrostatic at the COBR interface was evaluated using the developed TLM at both calcite–brine and oil–brine interfaces. The TLM predicted the trends and closely matched the magnitude of the measured  $\zeta$ -potential values. However, it should be noted that DLM is sufficient and in some cases better at predicting the  $\zeta$ -potential of rock–brine and oil–brine interfaces at the ionic strength used. This was because the DLM provides fewer parameters to be tuned and hence a less complex colloidal system. The DLM would be enough to capture the electrostatic interaction and reduce the modeling uncertainty. It was observed that the decreasing  $\text{Mg}^{2+}$  and increasing  $\text{SO}_4^{2-}$  concentrations decreased the  $\zeta$ -potential at the calcite–brine interface, shifting the polarity toward more negative. This observation was related to the effect of  $\text{Mg}^{2+}$  and  $\text{SO}_4^{2-}$  ion association at the calcite–brine interface. The increased adsorption of  $\text{SO}_4^{2-}$  was accompanied by a decreased  $>\text{CaOH}_2^+$  and  $>\text{CO}_3^-$  species at the surface. At high  $\text{SO}_4^{2-}$  concentrations, the negative species ( $>\text{CO}_3^-$  and  $>\text{CaSO}_4^-$ ) dominated the positive species ( $>\text{CaOH}_2^+$  and  $>\text{CO}_3^-$ ,  $\text{Mg}^+$ ) and hence made the calcite–brine interface more negative. At the oil–brine interface, the  $\text{Mg}^{2+}$  ion influenced the oil–brine interfaces, making the interface more negative with decreasing concentration. However,  $\text{SO}_4^{2-}$  had a lesser impact at the oil–brine interface, slightly making the interface more negative with increasing concentration, due to its nonreactive nature at the oil–brine interface.

The predicted  $\zeta$ -potential at both interfaces was used to calculate the total interaction potential according to the DLVO theory. A greater repulsive interaction potential was obtained for low  $\text{Mg}^{2+}$  and high  $\text{SO}_4^{2-}$  concentrations, which could result in altering carbonate wettability toward water wetness. The absolute sum of the  $\zeta$ -potential at both interfaces was observed to be logarithmically correlated to the total interaction potential at 0.25 separating distance. Thus, an increase in the absolute sum of  $\zeta$ -potential at both interfaces generated a greater repulsive interaction energy, which may trigger a water-wet surface and hence could be used as a screening parameter for field applications. The applicability of this screening parameter should be validated against contact angle measurements to confirm the wettability alteration since the predicted  $\zeta$ -potential was low using the MCB. It may be noted that more experimental and modeling data would be required to propose the specific  $\text{Mg}^{2+}$  and  $\text{SO}_4^{2-}$  ion concentrations to trigger wettability alteration, which would make this approach applicable to field situations.

## APPENDIX

## AUTHOR INFORMATION

### Corresponding Author

Joel T. Tetteh — School of Engineering, University of Kansas, Lawrence, Kansas 66045, United States; [orcid.org/0000-0001-5605-6861](https://orcid.org/0000-0001-5605-6861); Email: [joelteyetteh@gmail.com](mailto:joelteyetteh@gmail.com)

## Authors

Richard Barimah — School of Engineering, University of Kansas, Lawrence, Kansas 66045, United States

Paa Kow Korsah — Department of Petroleum Engineering, University of Wyoming, Laramie, Wyoming 82071, United States

Complete contact information is available at:

<https://pubs.acs.org/10.1021/acsomega.1c06954>

## Author Contributions

J.T.T.: Conceptualization, methodology, software, validation, formal analysis, investigation, data curation, writing—original draft preparation, and writing—review and editing. R.B.: Conceptualization, formal analysis, data curation, investigation, and writing—review and editing. P.K.K.: Conceptualization, formal analysis, and writing—review and editing. All authors have read and agreed to the published version of the manuscript.

## Funding

The authors received no funding for this work.

## Notes

The authors declare no competing financial interest.

## ACKNOWLEDGMENTS

The authors would like to express their immense gratitude to the anonymous reviewers whose valuable comments and suggestions improved the quality of this paper.

## REFERENCES

- (1) Yousef, A. A.; Al-Saleh, S. H.; Al-Kaabi, A.; Al-Jawfi, M. S. Laboratory Investigation of the Impact of Injection-Water Salinity and Ionic Content on Oil Recovery From Carbonate Reservoirs. *SPE Reservoir Eval. Eng.* **2011**, *14*, 578–593.
- (2) Nasralla, R. A.; Sergienko, E.; Masalmeh, S. K.; van der Linde, H. A.; Brussee, N. J.; Mahani, H.; Suijkerbuijk, B. M. J. M.; Al-Qarshubi, I. S. M. Potential of Low-Salinity Waterflood To Improve Oil Recovery in Carbonates: Demonstrating the Effect by Qualitative Coreflood. *SPE J.* **2016**, *21*, 1643–1654.
- (3) Austad, T.; Shariatpanahi, S. F.; Strand, S.; Aksulu, H.; Puntervold, T. Low Salinity EOR Effects in Limestone Reservoir Cores Containing Anhydrite: A Discussion of the Chemical Mechanism. *Energy Fuels* **2015**, *29*, 6903–6911.
- (4) Fathi, S. J.; Austad, T.; Strand, S. Water-Based Enhanced Oil Recovery (EOR) by “Smart Water”: Optimal Ionic Composition for EOR in Carbonates. *Energy Fuels* **2011**, *25*, 5173–5179.
- (5) Tetteh, J. T.; Brady, P. V.; Ghahfarokhi, R. B. Review of Low Salinity Waterflooding in Carbonate Rocks: Mechanisms, Investigation Techniques, and Future Directions. *Adv. Colloid Interface Sci.* **2020**, *284*, No. 102253.
- (6) Afekare, D. A.; Radonjic, M. From Mineral Surfaces and Coreflood Experiments to Reservoir Implementations: Comprehensive Review of Low-Salinity Water Flooding (LSWF). *Energy Fuels* **2017**, *31*, 13043–13062.
- (7) Korsah, P. K. *An Experimental Study of Engineered Water Flooding Solutions in a Tight Shaly Sandstone*; University of Wyoming, 2020.
- (8) Barimah, R. *Geochemical Feasibility of Brine Exchange Between Arbuckle and Lansing-Kansas City Formations as a Produced Water Management Alternative*; The University of Kansas, 2019.
- (9) Buckley, J. S.; Liu, Y.; Monsterleet, S. Mechanisms of Wetting Alteration by Crude Oils. *SPE J.* **1998**, *3*, 54–61.
- (10) Treiber, L. E.; Owens, W. W. A Laboratory Evaluation of the Wettability of Fifty Oil-Producing Reservoirs. *Soc. Pet. Eng. J.* **1972**, *12*, 531–540.
- (11) Tetteh, J. T.; Alimoradi, S.; Brady, P. V.; Barati Ghahfarokhi, R. Electrokinetics at Calcite-Rich Limestone Surface: Understanding the

Role of Ions in Modified Salinity Waterflooding. *J. Mol. Liq.* **2020**, *297*, No. 111868.

(12) Mahani, H.; Keya, A. L.; Berg, S.; Nasralla, R. Electrokinetics of Carbonate/Brine Interface in Low-Salinity Waterflooding: Effect of Brine Salinity, Composition, Rock Type, and PH on Zeta-Potential and a Surface-Complexation Model. *SPE J.* **2017**, *22*, 53–68.

(13) Fathi, S. J.; Austad, T.; Strand, S. “Smart Water” as a Wettability Modifier in Chalk: The Effect of Salinity and Ionic Composition. *Energy Fuels* **2010**, *24*, 2514–2519.

(14) Brady, P. V.; Thyne, G. Functional Wettability in Carbonate Reservoirs. *Energy Fuels* **2016**, *30*, 9217–9225.

(15) Hiorth, A.; Cathles, L. M.; Madland, M. V. The Impact of Pore Water Chemistry on Carbonate Surface Charge and Oil Wettability. *Transp. Porous Media* **2010**, *85*, 1–21.

(16) Zhang, P.; Tweheyo, M. T.; Austad, T. Wettability Alteration and Improved Oil Recovery by Spontaneous Imbibition of Seawater into Chalk: Impact of the Potential Determining Ions  $\text{Ca}^{2+}$ ,  $\text{Mg}^{2+}$ , and  $\text{SO}_4^{2-}$ . *Colloids Surf., A* **2007**, *301*, 199–208.

(17) Zhang, P.; Tweheyo, M. T.; Austad, T. Wettability Alteration and Improved Oil Recovery in Chalk: The Effect of Calcium in the Presence of Sulfate. *Energy Fuels* **2006**, *20*, 2056–2062.

(18) Rezaeidoust, A.; Puntervold, T.; Strand, S.; Austad, T. Smart Water as Wettability Modifier in Carbonate and Sandstone: A Discussion of Similarities/Differences in the Chemical Mechanisms. *Energy Fuels* **2009**, *23*, 4479–4485.

(19) Tetteh, J. T.; Brady, P. V.; Ghahfarokhi, R. B. Impact of Temperature and  $\text{SO}_4^{2-}$  on Electrostatic Controls over Carbonate Wettability. *Colloids Surf., A* **2021**, *625*, No. 126893.

(20) Song, J.; Wang, Q.; Shaik, I.; Puerto, M.; Bikina, P.; Aichele, C.; Biswal, S. L.; Hirasaki, G. J. Effect of Salinity,  $\text{Mg}^{2+}$  and  $\text{SO}_4^{2-}$  on “Smart Water”-Induced Carbonate Wettability Alteration in a Model Oil System. *J. Colloid Interface Sci.* **2020**, *563*, 145–155.

(21) Song, J.; Zeng, Y.; Wang, L.; Duan, X.; Puerto, M.; Chapman, W. G.; Biswal, S. L.; Hirasaki, G. J. Surface Complexation Modeling of Calcite Zeta Potential Measurements in Brines with Mixed Potential Determining Ions ( $\text{Ca}^{2+}$ ,  $\text{CO}_3^{2-}$ ,  $\text{Mg}^{2+}$ ,  $\text{SO}_4^{2-}$ ) for Characterizing Carbonate Wettability. *J. Colloid Interface Sci.* **2017**, *506*, 169–179.

(22) Song, J.; Rezaee, S.; Zhang, L.; Zhang, Z.; Puerto, M.; Wani, O. B.; Vargas, F.; Alhassan, S.; Biswal, S. L.; Hirasaki, G. J. Characterizing the Influence of Organic Carboxylic Acids and Inorganic Silica Impurities on the Surface Charge of Natural Carbonates Using an Extended Surface Complexation Model. *Energy Fuels* **2019**, *33*, 957–967.

(23) Chen, Y.; Xie, Q.; Sari, A.; Brady, P. V.; Saeedi, A. Oil/Water/Rock Wettability: Influencing Factors and Implications for Low Salinity Water Flooding in Carbonate Reservoirs. *Fuel* **2018**, *215*, 171–177.

(24) Xie, Q.; Sari, A.; Pu, W.; Chen, Y.; Brady, P. V.; Al Maskari, N.; Saeedi, A. PH Effect on Wettability of Oil/Brine/Carbonate System: Implications for Low Salinity Water Flooding. *J. Pet. Sci. Eng.* **2018**, *168*, 419–425.

(25) Xie, Q.; Brady, P. V.; Pooryousefy, E.; Zhou, D.; Liu, Y.; Saeedi, A. The Low Salinity Effect at High Temperatures. *Fuel* **2017**, *200*, 419–426.

(26) Erzuah, S.; Fjelde, I.; Omekeh, A. V. Wettability Estimation Using Surface-Complexation Simulations. *SPE Reservoir Eval. Eng.* **2019**, *22*, 509–519.

(27) Tetteh, J. T.; Veisi, M.; Brady, P. V.; Barati Ghahfarokhi, R. Surface Reactivity Analysis of the Crude Oil–Brine–Limestone Interface for a Comprehensive Understanding of the Low-Salinity Waterflooding Mechanism. *Energy Fuels* **2020**, *34*, 2739–2756.

(28) Goldberg, S.; Criscenti, L. J.; Turner, D. R.; Davis, J. A.; Cantrell, K. J. Adsorption-Desorption Processes in Subsurface Reactive Transport Modeling. *Vadose Zone J.* **2007**, *6*, 407–435.

(29) Goldberg, S. Adsorption Models Incorporated into Chemical Equilibrium Models. In *Chemical Equilibrium and Reaction Models*; Wiley, 1995.

(30) Takeya, M.; Shimokawara, M.; Elakneswaran, Y.; Nawa, T.; Takahashi, S. Predicting the Electrokinetic Properties of the Crude Oil/

Brine Interface for Enhanced Oil Recovery in Low Salinity Water Flooding. *Fuel* **2019**, *235*, 822–831.

(31) Heberling, F.; Bosbach, D.; Eckhardt, J. D.; Fischer, U.; Glowacky, J.; Haist, M.; Kramar, U.; Loos, S.; Müller, H. S.; Neumann, T.; Pust, C.; Schäfer, T.; Stelling, J.; Ukrainczyk, M.; Vinograd, V.; Vučak, M.; Winkler, B. Reactivity of the Calcite-Water-Interface, from Molecular Scale Processes to Geochemical Engineering. *Appl. Geochem.* **2014**, *45*, 158–190.

(32) Heberling, F.; Eng, P.; Lützenkirchen, J.; Trainor, T. P.; Bosbach, D.; Denecke, M. A. Structure and Reactivity of the Calcite–Water Interface. *J. Colloid Interface Sci.* **2011**, *354*, 843–857.

(33) Ding, H. *Investigating the Effects of  $\text{Ca}^{2+}$ ,  $\text{Mg}^{2+}$  and  $\text{SO}_4^{2-}$  on the Wettability of Carbonate Rocks*; The University of New South Wales, 2019.

(34) Ding, H.; Rahman, S. R. Investigation of the Impact of Potential Determining Ions from Surface Complexation Modeling. *Energy Fuels* **2018**, *32*, 9314–9321.

(35) Sanaei, A.; Tavassoli, S.; Sepehrnoori, K. Investigation of Modified Water Chemistry for Improved Oil Recovery: Application of DLVO Theory and Surface Complexation Model. *Colloids Surf., A* **2019**, *574*, 131–145.

(36) Brady, P. V.; Morrow, N. R.; Fogden, A.; Deniz, V.; Loahardjo, N.; Winoto, A. Electrostatics and the Low Salinity Effect in Sandstone Reservoirs. *Energy Fuels* **2015**, *29*, 666–677.

(37) Mahani, H.; Keya, A. L.; Berg, S.; Bartels, W. B.; Nasralla, R.; Rossen, W. R. Insights into the Mechanism of Wettability Alteration by Low-Salinity Flooding (LSF) in Carbonates. *Energy Fuels* **2015**, *29*, 1352–1367.

(38) Sanaei, A.; Tavassoli, S.; Sepehrnoori, K. Investigation of Modified Water Chemistry for Improved Oil Recovery: Application of DLVO Theory and Surface Complexation Model. *Colloids Surf., A* **2019**, *574*, 131–145.

(39) Bordeaux-Rego, F.; Mehrabi, M.; Sanaei, A.; Sepehrnoori, K. Improvements on Modelling Wettability Alteration by Engineered Water Injection: Surface Complexation at the Oil/Brine/Rock Contact. *Fuel* **2021**, *284*, No. 118991.

(40) Chandrasekhar, S.; Sharma, H.; Mohanty, K. K. Dependence of Wettability on Brine Composition in High Temperature Carbonate Rocks. *Fuel* **2018**, *225*, 573–587.

(41) Sharma, H.; Mohanty, K. K. An Experimental and Modeling Study to Investigate Brine-Rock Interactions during Low Salinity Water Flooding in Carbonates. *J. Pet. Sci. Eng.* **2018**, *165*, 1021–1039.

(42) Mohanty, K. K.; Chandrasekhar, S. In *Wettability Alteration with Brine Composition in High Temperature Carbonate Reservoirs*, SPE Annual Technical Conference and Exhibition; Society of Petroleum Engineers, 2013.

(43) Guo, H.; Nazari, N.; Esmaeilzadeh, S.; Kovscek, A. R. A Critical Review of the Role of Thin Liquid Films for Modified Salinity Brine Recovery Processes. *Curr. Opin. Colloid Interface Sci.* **2020**, *50*, No. 101393.

(44) Bartels, W.-B.; Mahani, H.; Berg, S.; Hassanzadeh, S. M. Literature Review of Low Salinity Waterflooding from a Length and Time Scale Perspective. *Fuel* **2019**, *236*, 338–353.

(45) Al Maskari, N. S.; Sari, A.; Saeedi, A.; Xie, Q. Influence of Surface Roughness on the Contact Angle Due to Calcite Dissolution in an Oil–Brine–Calcite System: A Nanoscale Analysis Using Atomic Force Microscopy and Geochemical Modeling. *Energy Fuels* **2019**, *33*, 4219–4224.

(46) Sari, A.; Al Maskari, N. S.; Saeedi, A.; Xie, Q. Impact of Surface Roughness on Wettability of Oil-Brine-Calcite System at Sub-Pore Scale. *J. Mol. Liq.* **2020**, *299*, No. 112107.

(47) Khishvand, M.; Alizadeh, A. H.; Kohshour, I. O.; Piri, M.; Prasad, R. S. In Situ Characterization of Wettability Alteration and Displacement Mechanisms Governing Recovery Enhancement Due to Low-Salinity Waterflooding. *Water Resour. Res.* **2017**, *53*, 4427–4443.

(48) Tetteh, J. T.; Cudjoe, S. E.; Aryana, S. A.; Barati Ghahfarokhi, R. Investigation into Fluid-Fluid Interaction Phenomenon during Low Salinity Waterflooding Using a Reservoir-on-a-Chip Microfluidics Model. *J. Pet. Sci. Eng.* **2020**, *196*, No. 108074.

- (49) Mohammadi, M.; Mahani, H. Direct Insights into the Pore-Scale Mechanism of Low-Salinity Waterflooding in Carbonates Using a Novel Calcite Microfluidic Chip. *Fuel* **2020**, *260*, No. 116374.
- (50) Sandengen, K.; Kristoffersen, A.; Melhuus, K.; Josang, L. O. Osmosis as Mechanism for Low-Salinity Enhanced Oil Recovery. *SPE J.* **2016**, *21*, 1227–1235.
- (51) Mohammadi, M.; Nikbin-Fashkacheh, H.; Mahani, H. Pore Network-Scale Visualization of the Effect of Brine Composition on Sweep Efficiency and Speed of Oil Recovery from Carbonates Using a Photolithography-Based Calcite Microfluidic Model. *J. Pet. Sci. Eng.* **2022**, *208*, No. 109641.
- (52) Shaik, I. K.; Zhang, L.; Pradhan, S.; Kalkan, A. K.; Aichele, C. P.; Bikina, P. K. A Parametric Study of Layer-by-Layer Deposition of CaCO<sub>3</sub> on Glass Surfaces towards Fabricating Carbonate Reservoirs on Microfluidic Chips. *J. Pet. Sci. Eng.* **2021**, *198*, No. 108231.
- (53) Liu, S.; Zhang, C.; Ghahfarokhi, R. B. A Review of Lattice-Boltzmann Models Coupled with Geochemical Modeling Applied for Simulation of Advanced Waterflooding and Enhanced Oil Recovery Processes. *Energy Fuels* **2021**, *35*, 13535–13549.
- (54) Tetteh, J. T. In *Nano to Macro Scale Investigation into Low Salinity Waterflooding in Carbonate Rocks*, SPE Annual Technical Conference and Exhibition; Society of Petroleum Engineers, 2020. <https://doi.org/10.2118/204276-STU>.
- (55) Pourakaberian, A.; Mahani, H.; Niasar, V. The Impact of the Electrical Behavior of Oil-Brine-Rock Interfaces on the Ionic Transport Rate in a Thin Film, Hydrodynamic Pressure, and Low Salinity Waterflooding Effect. *Colloids Surf., A* **2021**, *620*, No. 126543.
- (56) Appelo, C. A. J.; Postma, D. Hydrogeochemical Modeling with PHREEQC. In *Geochemistry, Groundwater and Pollution*, 2nd ed.; A.A. Balkema Publishers, 2005; Vol. 59.
- (57) Appelo, C.; Postma, D. Hydrogeochemical Modeling with PHREEQC. In *Geochemistry, Groundwater and Pollution*; CRC Press, 2010.
- (58) Brady, P. V.; Krumhansl, J. L.; Mariner, P. E. In *Surface Complexation Modeling for Improved Oil Recovery*, SPE Improved Oil Recovery Symposium; Society of Petroleum Engineers, 2012; pp 14–18.
- (59) Chen, Y.; Sari, A.; Xie, Q.; Brady, P. V.; Hossain, M. M.; Saeedi, A. Electrostatic Origins of CO<sub>2</sub>-Increased Hydrophilicity in Carbonate Reservoirs. *Sci. Rep.* **2018**, *8*, No. 17691.
- (60) Song, J.; Wang, Q.; Shaik, I.; Puerto, M.; Bikina, P.; Aichele, C.; Biswal, S. L.; Hirasaki, G. J. Effect of Salinity, Mg<sup>2+</sup> and SO<sub>4</sub><sup>2-</sup> on “Smart Water”-Induced Carbonate Wettability Alteration in a Model Oil System. *J. Colloid Interface Sci.* **2020**, *563*, 145–155.
- (61) Sanaei, A.; Tavassoli, S.; Sepahmooi, K. Investigation of Modified Water Chemistry for Improved Oil Recovery: Application of DLVO Theory and Surface Complexation Model. *Colloids Surf., A* **2018**, *574*, 131–145.
- (62) Bonto, M.; Eftekhari, A. A.; Nick, H. M. An Overview of the Oil-Brine Interfacial Behavior and a New Surface Complexation Model. *Sci. Rep.* **2019**, *9*, No. 6072.
- (63) Bonto, M.; Eftekhari, A. A.; M Nick, H. Wettability Indicator Parameter Based on the Thermodynamic Modeling of Chalk-Oil-Brine Systems. *Energy Fuels* **2020**, *34*, 8018–8036.
- (64) Bonto, M.; Eftekhari, A. A.; Nick, H. In *A Calibrated Model for the Carbonate-Brine-Crude Oil Surface Chemistry and Its Effect on the Rock Wettability, Dissolution, and Mechanical Properties*, SPE Reservoir Simulation Conference; OnePetro, 2019.
- (65) Eftekhari, A. A.; Thomsen, K.; Stenby, E. H.; Nick, H. M. Thermodynamic Analysis of Chalk-Brine-Oil Interactions. *Energy Fuels* **2017**, *31*, 11773–11782.
- (66) Wolthers, M.; Charlet, L.; Van Cappellen, P. The Surface Chemistry of Divalent Metal Carbonate Minerals: A Critical Assessment of Surface Charge and Potential Data Using the Charge Distribution Multi-Site Ion Complexation Model. *Am. J. Sci.* **2008**, *308*, 905–941.
- (67) Takeya, M.; Ubaidah, A.; Shimokawara, M.; Okano, H.; Nawa, T.; Elakneswaran, Y. Crude Oil/Brine/Rock Interface in Low Salinity Waterflooding: Experiments, Triple-Layer Surface Complexation Model, and DLVO Theory. *J. Pet. Sci. Eng.* **2020**, *188*, No. 106913.
- (68) Purswani, P.; Karpyn, Z. T. Laboratory Investigation of Chemical Mechanisms Driving Oil Recovery from Oil-Wet Carbonate Rocks. *Fuel* **2019**, *235*, 406–415.
- (69) Zhang, P.; Austad, T. Wettability and Oil Recovery from Carbonates: Effects of Temperature and Potential Determining Ions. *Colloids Surf., A* **2006**, *279*, 179–187.
- (70) Mansi, M.; Mehana, M.; Fahes, M.; Viswanathan, H. Thermodynamic Modeling of the Temperature Impact on Low-Salinity Waterflooding Performance in Sandstones. *Colloids Surf., A* **2020**, *586*, No. 124207.
- (71) Khurshid, I.; Al-Shalabi, E. W. New Insights into Modeling Disjoining Pressure and Wettability Alteration by Engineered Water: Surface Complexation Based Rock Composition Study. *J. Pet. Sci. Eng.* **2022**, *208*, No. 109584.
- (72) Korrani, A. K. N.; Jerauld, G. R. In *Modeling Wettability Change in Sandstones and Carbonates Using a Surface-Complexation-Based Method*, SPE Improved Oil Recovery Conference; Society of Petroleum Engineers, 2018. <https://doi.org/10.2118/190236-MS>.
- (73) Israelachvili, J. N. *Intermolecular and Surface Forces*; Elsevier, 2011; Vol. 3.
- (74) Maghsoudian, A.; Esfandiarian, A.; Kord, S.; Tamsilian, Y.; Soulgani, B. S. Direct Insights into the Micro and Macro Scale Mechanisms of Symbiotic Effect of SO<sub>4</sub><sup>2-</sup>, Mg<sup>2+</sup>, and Ca<sup>2+</sup> Ions Concentration for Smart Waterflooding in the Carbonated Coated Micromodel System. *J. Mol. Liq.* **2020**, *315*, No. 113700.
- (75) Alshakhs, M. J.; Kovscek, A. R. Understanding the Role of Brine Ionic Composition on Oil Recovery by Assessment of Wettability from Colloidal Forces. *Adv. Colloid Interface Sci.* **2016**, *233*, 126–138.
- (76) Xie, Q.; Liu, F.; Chen, Y.; Yang, H.; Saeedi, A.; Hossain, M. M. Effect of Electrical Double Layer and Ion Exchange on Low Salinity EOR in a PH Controlled System. *J. Pet. Sci. Eng.* **2019**, *174*, 418–424.
- (77) Takeya, M.; Shimokawara, M.; Elakneswaran, Y.; Okano, H.; Nawa, T. Effect of Acid Number on the Electrokinetic Properties of Crude Oil during Low-Salinity Waterflooding. *Energy Fuels* **2019**, *33*, 4211–4218.
- (78) Ding, H.; Mettu, S.; Rahman, S. S. Impacts of Smart Waters on Calcite-Crude Oil Interactions Quantified by “Soft Tip” Atomic Force Microscopy (AFM) and Surface Complexation Modeling (SCM). *Ind. Eng. Chem. Res.* **2020**, *59*, 20337–20348.
- (79) Stipp, S. L. S. Toward a Conceptual Model of the Calcite Surface: Hydration, Hydrolysis, and Surface Potential. *Geochim. Cosmochim. Acta* **1999**, *63*, 3121–3131.
- (80) Hao, X.; Abu-Al-Saud, M.; Ayrala, S.; Elakneswaran, Y. Influence of Carbonate Impurities on Smartwater Effect: Evaluation of Wettability Alteration Process by Geochemical Simulation. *J. Mol. Liq.* **2021**, *340*, No. 117165.
- (81) Saeed, M.; Jadhawar, P.; Zhou, Y.; Abhishek, R. Triple-Layer Surface Complexation Modelling: Characterization of Oil-Brine Interfacial Zeta Potential under Varying Conditions of Temperature, PH, Oil Properties and Potential Determining Ions. *Colloids Surf., A* **2022**, *633*, No. 127903.
- (82) Elakneswaran, Y.; Ubaidah, A.; Takeya, M.; Shimokawara, M.; Okano, H. Effect of Electrokinetics and Thermodynamic Equilibrium on Low-Salinity Water Flooding for Enhanced Oil Recovery in Sandstone Reservoirs. *ACS Omega* **2021**, *6*, 3727–3735.
- (83) Taheriotagsara, M.; Bonto, M.; Nick, H. M.; Eftekhari, A. A. Estimation of Calcite Wettability Using Surface Forces. *J. Ind. Eng. Chem.* **2021**, *98*, 444–457.
- (84) Vinogradov, J.; Hidayat, M.; Sarmadivaleh, M.; Derksen, J.; Vega-Maza, D.; Iglauer, S.; Jougnot, D.; Azaroual, M.; Leroy, P. Predictive Surface Complexation Model of the Calcite-Aqueous Solution Interface: The Impact of High Concentration and Complex Composition of Brines. *J. Colloid Interface Sci.* **2021**, *609*, 852–867.
- (85) Ding, H.; Mettu, S.; Rahman, S. Probing the Effects of Ca<sup>2+</sup>, Mg<sup>2+</sup>, and SO<sub>4</sub><sup>2-</sup> on Calcite-Oil Interactions by “Soft Tip” Atomic Force Microscopy (AFM). *Ind. Eng. Chem. Res.* **2020**, *59*, 13069–13078.

- (86) Boampong, L. O.; Rafati, R.; Sharifi Haddad, A. A Calibrated Surface Complexation Model for Carbonate-Oil-Brine Interactions Coupled with Reservoir Simulation—Application to Controlled Salinity Water Flooding. *J. Pet. Sci. Eng.* **2022**, *208*, No. 109314.
- (87) Tetteh, J. T.; Pham, A.; Peltier, E.; Hutchison, J. M.; Barati Ghahfarokhi, R. Predicting the Electrokinetic Properties on an Outcrop and Reservoir Composite Carbonate Surfaces in Modified Salinity Brines Using Extended Surface Complexation Models. *Fuel* **2022**, *309*, No. 122078.
- (88) Mahani, H.; Menezes, R.; Berg, S.; Fadili, A.; Nasralla, R.; Voskov, D.; Joekar-Niasar, V. Insights into the Impact of Temperature on the Wettability Alteration by Low Salinity in Carbonate Rocks. *Energy Fuels* **2017**, *31*, 7839–7853.
- (89) Ding, H.; Rahman, S. Experimental and Theoretical Study of Wettability Alteration during Low Salinity Water Flooding—an State of the Art Review. *Colloids Surf., A* **2017**, *520*, 622–639.
- (90) Myint, P. C.; Firoozabadi, A. Thin Liquid Films in Improved Oil Recovery from Low-Salinity Brine. *Curr. Opin. Colloid Interface Sci.* **2015**, *20*, 105–114.
- (91) Hirasaki, G. J. Wettability: Fundamentals and Surface Forces. *SPE Form. Eval.* **1991**, *6*, 217–226.
- (92) Gregory, J. Interaction of Unequal Double Layers at Constant Charge. *J. Colloid Interface Sci.* **1975**, *51*, 44–51.
- (93) Hough, D. B.; White, L. R. The Calculation of Hamaker Constants from Lifshitz Theory with Applications to Wetting Phenomena. *Adv. Colloid Interface Sci.* **1980**, *14*, 3–41.
- (94) Shalabi, E. W. A. *Modeling the Effect of Injecting Low Salinity Water on Oil Recovery from Carbonate Reservoirs*; University of Texas at Austin, 2014.
- (95) Brady, P. V.; Krumhansl, J. L. A Surface Complexation Model of Oil–Brine–Sandstone Interfaces at 100°C: Low Salinity Waterflooding. *J. Pet. Sci. Eng.* **2012**, *81*, 171–176.
- (96) Guo, H.; Kovscek, A. R. Investigation of the Effects of Ions on Short-Range Non-DLVO Forces at the Calcite/Brine Interface and Implications for Low Salinity Oil-Recovery Processes. *J. Colloid Interface Sci.* **2019**, *552*, 295–311.
- (97) Mehana, M.; Fahes, M.; Kang, Q.; Viswanathan, H. Molecular Simulation of Double Layer Expansion Mechanism during Low-Salinity Waterflooding. *J. Mol. Liq.* **2020**, *318*, No. 114079.
- (98) Lee, S. Y.; Webb, K. J.; Collins, I.; Lager, A.; Clarke, S.; O’Sullivan, M.; Routh, A.; Wang, X. In *Low Salinity Oil Recovery: Increasing Understanding of the Underlying Mechanisms*, SPE Improved Oil Recovery Symposium; OnePetro, 2010.
- (99) Sari, A.; Xie, Q.; Chen, Y.; Saeedi, A.; Pooryousefy, E. Drivers of Low Salinity Effect in Carbonate Reservoirs. *Energy Fuels* **2017**, *31*, 8951–8958.
- (100) Ding, H.; Wang, Y.; Shapoval, A.; Zhao, Y.; Rahman, S. Macro- and Microscopic Studies of “Smart Water” Flooding in Carbonate Rocks: An Image-Based Wettability Examination. *Energy Fuels* **2019**, *33*, 6961–6970.
- (101) Hao, J.; Mohammadkhani, S.; Shahverdi, H.; Esfahany, M. N.; Shapiro, A. Mechanisms of Smart Waterflooding in Carbonate Oil Reservoirs—A Review. *J. Pet. Sci. Eng.* **2019**, *179*, 276–291.
- (102) Mitchell, R. W.; Grist, D. M.; Boyle, M. J. Chemical Treatments Associated With North Sea Projects. *J. Pet. Technol.* **2007**, *35*, 904–912.
- (103) Yousef, A. A.; Liu, J. S.; Blanchard, G. W.; Al-Saleh, S.; Al-Zahrani, T.; Al-Zahrani, R. M.; Al-Tammar, H. I.; Al-Mulhim, N. In *Smart Waterflooding: Industry*, SPE Annual Technical Conference and Exhibition; Society of Petroleum Engineers, 2012; pp 8–10.
- (104) Zhang, P.; Austad, T. Wettability and Oil Recovery from Carbonates: Effects of Temperature and Potential Determining Ions. *Colloids Surf., A* **2006**, *279*, 179–187.